Gravity waves in the middle atmosphere observed by Rayleigh lidar: 2. Climatology

Richard Wilson, Marie-Lise Chanin, Alain Hauchecorne

JOURNAL OF GEOPHYSICAL RESEARCH, VOL. 96, NO. D3, PAGES 5169–5183, MARCH 20, 1991

GRAVITY WAVES IN THE MIDDLE ATMOSPHERE OBSERVED BY RAYLEIGH LIDAR 2. CLIMATOLOGY

R. Wilson, M. L. Chanin, and A. Hauchecorne

Service D'Aéronomie du CNRS, Verrieres le Buisson, France

Abstract. A large data set obtained by Rayleigh lidars during 4 years has been analyzed in order to describe the gravity wave climatology in the 30- to 75-km altitude range at mid-latitude. The lidar data were collected in two sites different with respect to orography, both located in the south of France (44°N). The seasonal variability of the wave activity, the vertical growth of potential energy density per unit mass, and the power spectral density versus vertical wave number are shown. The seasonal variability of the wave activity is found to be mainly annual, the maximum of activity occurring during winter. A semiannual component, with a secondary maximum in summer, is superposed to the annual cycle above 60-km altitude. The power spectral density increases from the stratosphere to the mesosphere in the entire spectral range. A significant positive correlation is found between the wave activity and the wind intensity in the stratosphere. Finally, some simple hypotheses, in terms of wave sources and wave transmission, are advanced in order to get an insight into the causes of the observed seasonal and geographical variability of the wave activity.

1. Introduction

Routine lidar measurements performed at two stations located in the south of France, at the Observatoire de Haute Provence (OHP) (44°N, 6°E) and at Biscarosse (BIS) (44°N, 1°W), during 4 years, from 1986 to 1989, provide a large data base to study the mesoscale variability of the middle atmosphere. The mesoscale fluctuations are interpreted in the framework of the internal gravity wave theory. Through momentum and energy transport and deposition, gravity waves are thought to play a major role in the large-scale dynamics and thermal budget of the middle atmosphere. The convergence of the momentum and energy fluxes transported by internal gravity waves largely induce the mean zonal and meridional circulation, and thus the temperature distribution, as well as the turbulent diffusion of heat and constituents, in the mesosphere [Lindzen 1981; Matsuno, 1982; Holton, 1982; Garcia and Solomon, 1985, Strobel et al., 1985] and in the stratosphere [Palmer et al., 1986; Miyahara et al., 1986; Tanaka, 1986]. Moreover, large temperature inversions frequently observed in the mesosphere, which could persist several days, are likely to be induced by gravity wave breaking [Hauchecorne et al., 1987; Hauchecorne and Maillard, 1990]. A climatological description of the gravity wave activity is therefore crucial to the understanding of the large scale dynamic of the middle atmosphere.

Case studies [Wilson et al., this issue] (hereinafter WCH) have shown that the day-to-day variability of the wave energy density per unit mass in a given altitude range is very large, within a factor of 5 in the stratosphere, and up to 1 order of magnitude in the mesosphere. Beyond the description of the gravity wave field drawn from recurrently observed patterns from case studies, the purpose of this paper is to describe the mean features of the gravity wave field at mid-latitudes as a function of season and altitude, from a large data set. This represents the first extensive study of the gravity waves field in this height range by use of the lidar technique. The seasonal variability of the wave activity, the typical energy levels as a function of altitude, the systematic differences between the two sites in the stratosphere and mesosphere will be described and discussed. Finally, some hypotheses, in terms of orographic sources and background wind filtering will be advanced to interpret the observed seasonal and geographical variability of the wave activity.

This paper is organized as follows. The data base is described in section 2. The seasonal variability of the wave activity, the vertical growth of potential energy and the mean power spectral density (PSD) of gravity waves in the stratosphere and mesosphere are shown in section 3. The results are discussed in section 4: first, a comparison of the present results with other gravity wave climatologies is presented; then, some hypotheses are advanced in order to interpret the observed seasonal variation. Conclusions are summarized in section 5.

2. The Data Base: Description and Processing

Rayleigh lidar measurements give access to the relative perturbations of density ρ'/ρ_0 (or temperature T'/T_0), to the mean static stability (the Brunt-Väisälä frequency, N), and therefore to the available potential energy density per unit mass, E_p (for more details see Chanin and Hauchecorne [1981, 1984] and WCH). Indeed, the potential energy per unit mass, E_p, is

$$E_p = \frac{1}{2} N^2 \langle \xi^2 \rangle = \frac{1}{2} \left(\frac{g}{N}\right)^2 \left\langle \left(\frac{\rho'}{\rho_0}\right)^2 \right\rangle \quad (1)$$

where ξ is the vertical displacement of an air parcel, N the

Paper number 90JD02610.
0148-0227/91/90JD-02610$05.00

Brunt-Väisälä frequency, and g the Earth acceleration. The term "activity" as used in this paper refers to the available potential energy density per unit mass, Ep, expressed in joules per kilogramme.

The vertical wavelength of a gravity wave is related to the intrinsic phase speed (there is no Doppler shift bias). The saturation amplitude, i.e., the amplitude over which convective or dynamical instabilities occur is also a function of the vertical scale of the fluctuations. The PSD versus vertical wave number is thus directly comparable to the saturation limit predicted by the gravity waves theory [Dewan and Good, 1986; Smith et al., 1987]. Because the convective saturation amplitude of the density (or temperature) relative fluctuations, ρ'/ρ_0 (T'/T_0) is proportional to N^2/g [Dewan and Good, 1986], the perturbations for the spectral analysis are defined as $(g/N^2)(\rho'/\rho_0)$ in order to get a comparison from one spectrum to another with respect to the saturation limit independently of the mean temperature and/or static stability conditions. The white noise level of the lidar signal is evaluated in the high wave number portion of the spectrum (where the signal-to-noise ratio is close to unity), that is to say for vertical wavelengths shorter than 1 km. This noise level is then subtracted from the raw spectrum [WCH]. The spectral analysis is performed in three altitude ranges: the upper stratosphere from 30 to 45 km, the lower mesosphere, from 45 to 60 km (the mean stratopause level ranging between 45 and 48 km altitude), and the middle mesosphere (60 to 75 km). The density profiles have been obtained with 15-min integration time and 300-m spatial (vertical) resolution, giving thus access to (apparent) period larger than half an hour and to vertical scales larger than 600 m. The energy density per unit mass, Ep, is deduced integrating the density fluctuations PSD over vertical wave numbers from 1/15 to 1/0.6 km^{-1} and then scaling by the averaged value of N^2. The mean PSD, from which Ep is inferred, is averaged over all the individual spectra (deduced from 15-min integrated profiles) obtained during a given period (a day, or one or several months).

The potential energy growth as a function of altitude is estimated in three wavelength bands, centered on 10, 7.5, and 5 km, by mean of a complex demodulation of the perturbations profiles. The density fluctuations are normalized in this case as $(g/N)(\rho'/\rho_0)$, the variance of which is twice the potential energy of the fluctuations.

The climatological study relies upon 4 years of data collected at OHP, from 1986 to 1989, and 3 years and 9 months at BIS, the data being obtained at this site only since April 1986. Taking into account roughly 100 nights of measurements a year, each night duration being, in the average, of 3 to 4 hours, about 10,000 vertical profiles of density were used for this study. Nevertheless, a selection of data was performed. First, some vertical profiles obtained during stratospheric warming or mesospheric temperature inversions were eliminated to avoid introducing variance due to large scale motions. Then, an upper limit of the noise level for each sample of the averaged spectral estimator was fixed in the mesosphere, depending on the altitude domain, 45-60 or 60-75 km. Due to the exponential growth of the noise with altitude, the signal-to-noise ratio decreases from an average value of 2 in the upper stratosphere (30-45 km) to about 1.1 in the middle mesosphere (60-75 km). As a consequence the number of selected data becomes smaller with increasing altitude.

Unique features of this data set are first the large amount of available data in a barely explored height range and second the fact that the two sites of BIS and OHP, both at same latitude (44°N) and distant by 550 km, are differently located with respect to orography. The BIS station is situated on the Atlantic coast, with dominant westerly tropospheric wind, whereas the OHP is located in the foothills of the Alps, where the orographic sources are expected to be more intense.

3. Gravity Wave Climatology

3.1. Gravity Wave Activity

The seasonal variation of the wave activity is investigated using three different and complementary analyses which have been applied to the three height ranges defined above for both sites separately. First, the whole set of the daily estimations of the potential energy per unit mass, Ep, are shown for each site and for the three height ranges. These daily estimations of Ep are inferred from the daily averaged power spectra. A least squares fit by 12 sine and cosine functions with period ranging from 48 to 4 months is performed on the daily Ep values, giving an insight into the seasonal and interannual variability of the wave activity. The seasonal variation is then presented in a yearly sequence in order to reduce the gaps and inhomogeneity of the data set. A least squares fit by four periodic functions with periods of 12 to 3 months is performed on the Ep daily values. Finally, the monthly means of Ep, inferred from monthly averaged spectra, are shown with a $\pm 2\sigma$ error bar. These monthly mean PSDs, averaged over about 400 to 800 spectra, are performed in order to increase the accuracy of the signal-to-noise ratio and thus of the mean Ep estimations.

The seasonal variation of the wave activity in the upper stratosphere is shown in Figures 1, 2, and 3. An annual cycle is clearly evident at both sites with a maximum of activity occurring during winter and a minimum during summer. An interannual variability is observed at BIS (Figure 1): the winter maximum of the wave activity decreases from one year to another from about 10-12 j/kg to 6 j/kg. Nevertheless, this result could be biased owing to the temporal inhomogeneity of the data set. The day to day variability appears to be much larger during winter at both sites (Figures 1 and 2). The amplitude of the seasonal variation (a factor ranging between 2 and 3) is somewhat larger at OHP than at BIS (Figures 2 and 3). Indeed, the monthly mean of Ep (Figure 3) is larger during winter months at OHP (12 j/kg on average) than at Biscarosse (7 j/kg), whereas the difference is relatively small during summer (4 to 5 j/kg).

In the lower mesosphere (45 to 60 km) the same type of seasonal variation of the wave activity is observed (Figures 4, 5, 6) : the maximum occurs during winter, the minimum

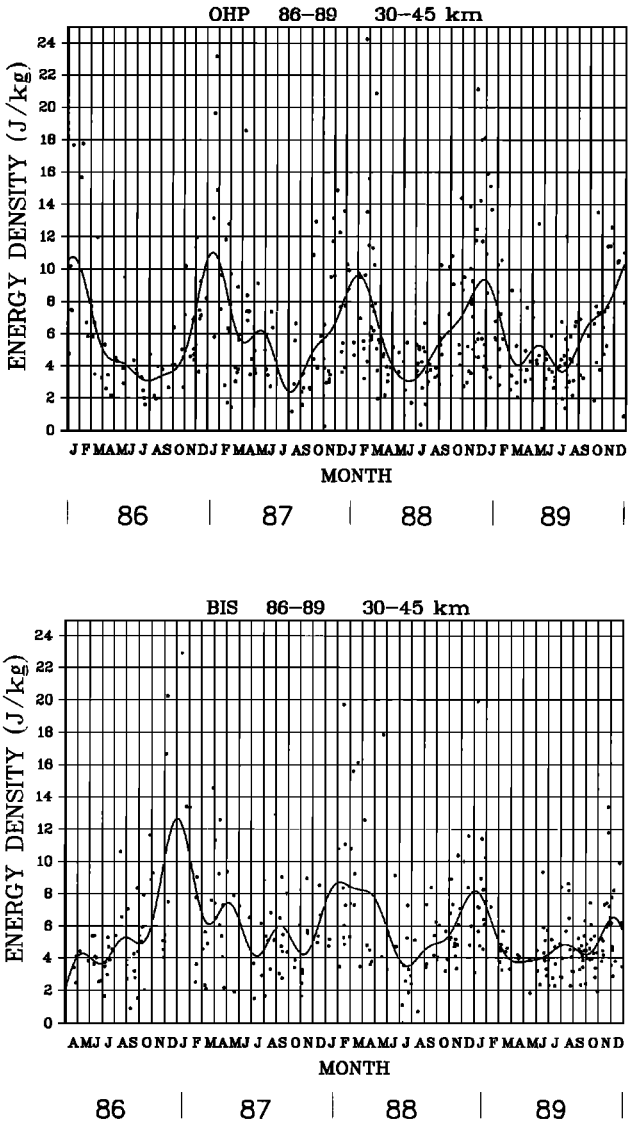

Fig. 1. Daily estimates of the potential energy density per unit mass in the upper stratosphere (30-45 km) from January (April) 1986 to December 1989 at (top) OHP and (bottom) BIS. A least squares fit by a linear combination of 12 sine and cosine functions (periods of 48 to 4 months) is performed on the daily estimations (smoothed curve).

during summer. A slight increase of the wave activity is observed at OHP for the years 1988-1989 which is not observed at BIS (Figure 4). The winter maximum of the wave activity presents often a double peak in October-November and January-February at OHP. The strong wave activity observed at OHP in October 1987, 1988, and 1989 is not seen at BIS. On the contrary, a relatively large activity is observed in April-May 1987 and 1988 at BIS which is not present at OHP (Figure 4). The wave activity is thus somewhat uncorrelated for the two sites distant from 550 km. The magnitude of the seasonal variation ranges between 1.5 (at OHP) and 2 (at BIS), and is thus weaker at OHP than it was at lower level. A more intense wave activity is observed at OHP, especially during summer (Figures 5 and 6).

In the middle mesosphere (60-75 km), the day-to-day variability of the wave activity seems to be large in all seasons (Figure 7). Such a dispersion of the daily Ep values is partly due to the increasing noise level. However, it appears that maxima occur not only in winter, from October to March, but also in June-July as observed at OHP in 1988-1989 and at BIS in 1987, 1988, and 1989. In the average, a semiannual variation of the wave activity is observed (Figures 8 and 9) with activity minima in May and September. The amplitude of the seasonal variation stays, as in the lower mesosphere, around a factor of 2 at BIS and 1.5 at OHP (Figure 9). Again, the wave activity in this height range is found to be larger at OHP than at BIS (from 10 to 30%), especially during summer (Figures 8 and 9).

To summarize, the seasonal variability of the gravity wave activity is mainly annual in the stratosphere and lower mesosphere, the maximum of activity occurring during winter, the minimum during summer at both sites. Above 60

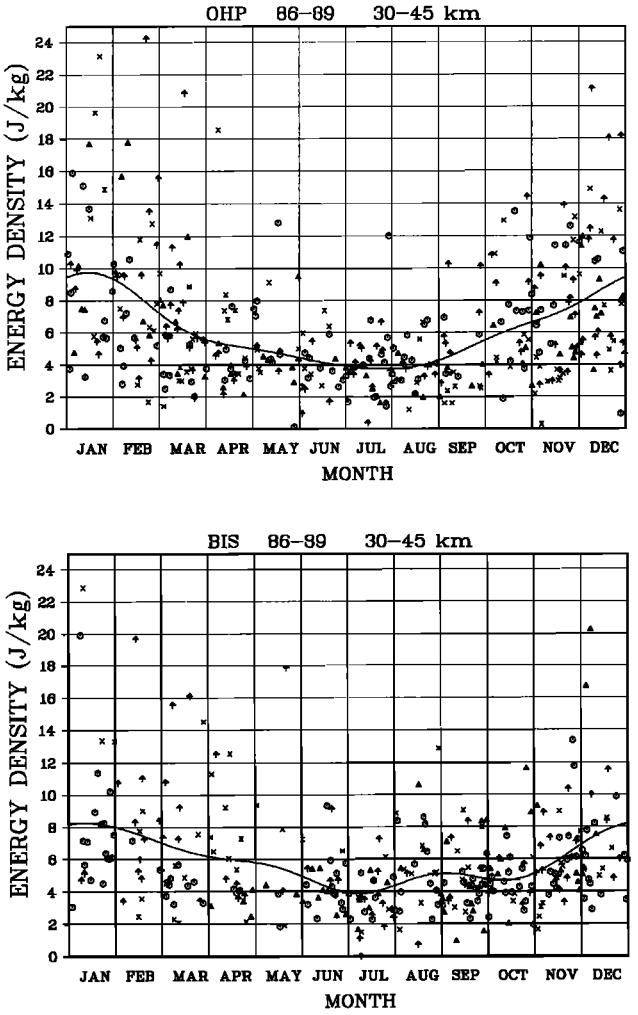

Fig. 2. Daily estimates of the potential energy density per unit mass in the upper stratosphere (30-45 km) observed during 4 years (86 to 89) and reduced into 1 year. A least squares fit by a linear combination of four sine and cosine functions (period of 12 to 3 months) is performed (smoothed curve).

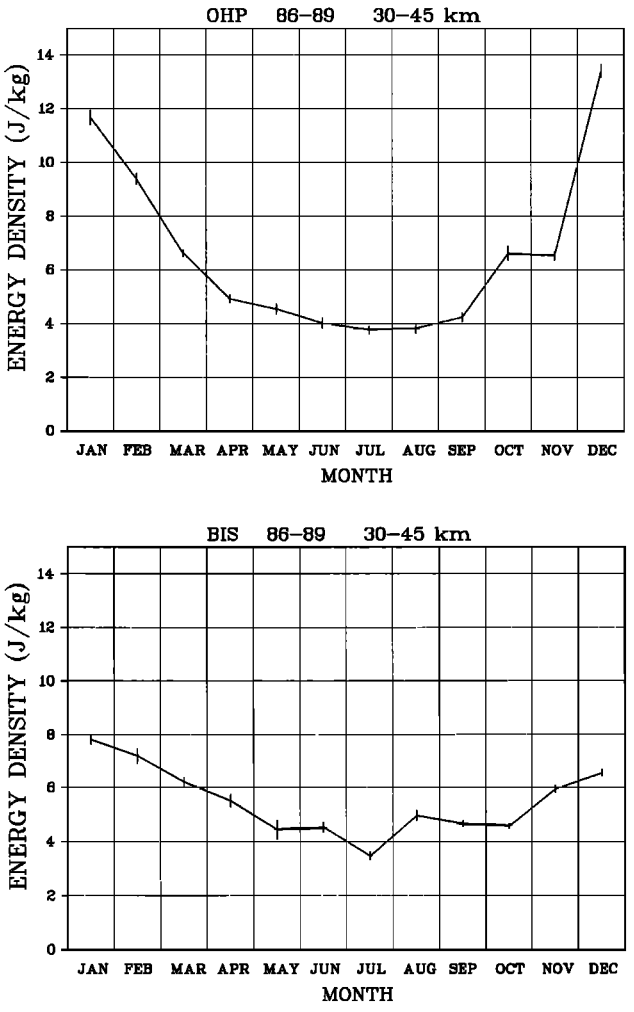

Fig. 3. The monthly means of the potential energy density per unit mass at OHP and BIS deduced from the integrated mean vertical spectrum of the normalized density fluctuations. The monthly mean spectrum is averaged over the spectra (from 15 min integrated density profiles) obtained during 4 years.

km altitude, a semiannual component of the wave activity, superimposed on the annual cycle, is observed : a secondary maximum, more pronounced at OHP, occurs during summer.

3.2. The Potential Energy Density Versus Altitude

The energy growth versus altitude can be roughly inferred from the ratio of potential energy density per unit mass in the various height ranges. From the upper stratosphere to the lower mesosphere (Figures 3 and 6), the mean energy growth rate ranges between 2 and 6 over about 2 density scale heights. The largest energy growth, about a factor of 4 to 6, is observed during summer at OHP, whereas the smaller one is observed during winter at OHP and during summer at BIS (between 2 and 3). The energy scale height, H_E (= $\Delta z/\ln\{Ep(z+\Delta z)/Ep(z)\}$), thus ranges between 8.5 and 20 km in the 30- to 60-km height range. These relatively large energy scale heights suggest an energy and momentum deposition in the upper stratosphere and lower mesosphere, even though background wind shears can conservatively reduce (or enhance) the wave growth with height [WCH]. However, the results are basically the same during weak background flow (April-May and September), that is to say, when the background wind shear effects should be minimum ($12<H_E<16$ km). From the lower to the middle mesosphere (Figures 6 and 9), the energy growth rate seems relatively larger that at lower level: from a factor of 4 (during winter at OHP) to 8 (during summer at BIS) over about 2.5 density scale heights. The energy scale height thus ranges between 7 and 10 km in the mesosphere (45 to 75 km). Nevertheless, this last result could be partially biased owing to the filtering of low Ep values in the middle mesosphere due to the decreasing signal-to-noise ratio.

The Ep vertical growth of the large vertical scale fluctuations has been studied in more detail by using a

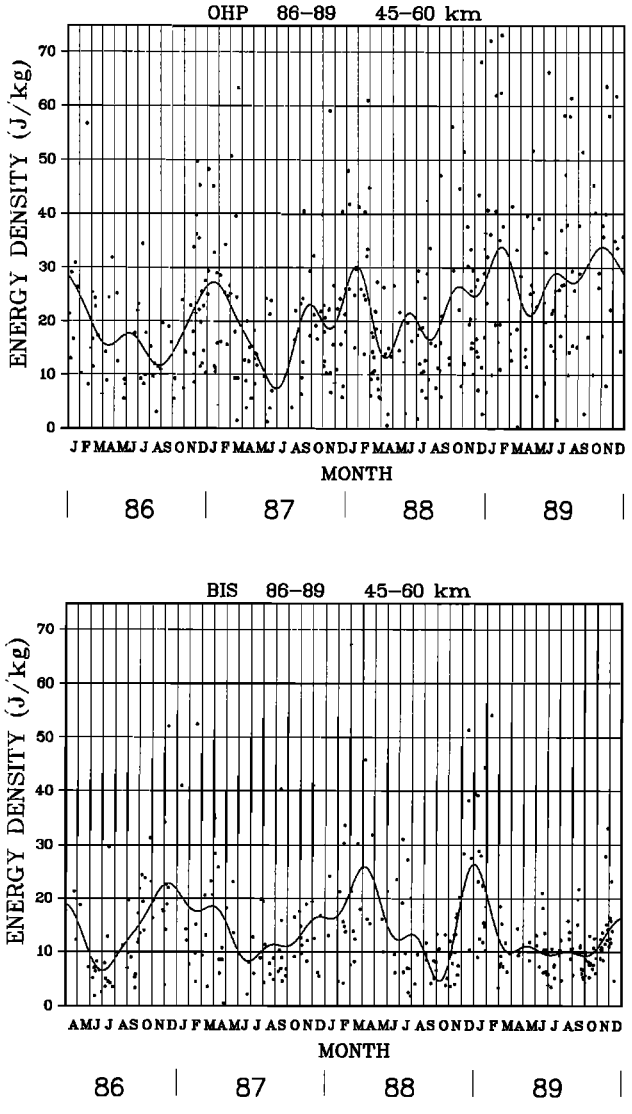

Fig. 4. The same as Figure 1 except in the lower mesosphere (45 to 60 km)

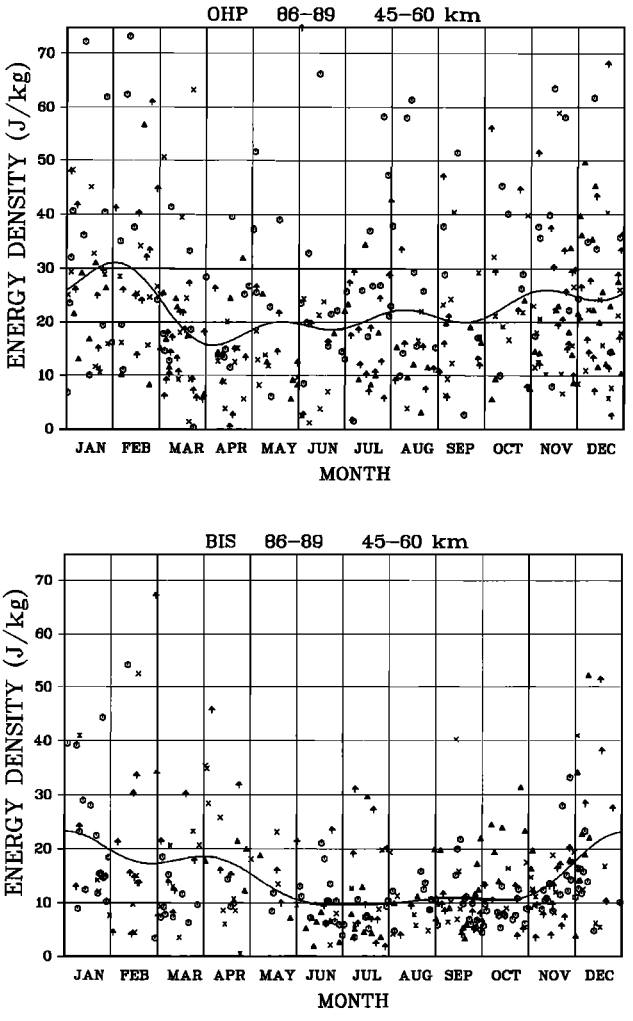

Fig. 5. The same as Figure 2 except in the lower mesosphere (45 to 60 km)

complex demodulation of the perturbed density profiles in three wavelength bands (centered on 10, 7.5, and 5 km). The vertical growth of the energy density is shown in Figures 10 (OHP) and 11 (BIS). The seasonal mean of the potential energy density has been averaged over winter months (December, January, and February), summer months (June, July, August), and equinox months, i.e., in relatively weak wind conditions (April, May, and September). A mean vertical scale height (7 km) as well as the noise level, estimated on short vertical scales (1 km and less), are plotted for comparison. Notice that the noise level is higher by about a factor of 2 at OHP than at BIS. In any case the vertical growth rate of Ep is weak, a factor of 5 or less (H_E>13 km), in the 35 to 55-60 km height range. Above 60-km altitude, the energy growth rate may increase as seen at BIS both in summer for the 10- to 7.5-km vertical scale motions (7.5<H_E<13 km) and in winter for the 5-km vertical scale motions (H_E≈8 km). During equinox the energy growth rate remains nearly constant in the entire height range from 35 to 75 km (15<H_E<23 km). The same behavior is observed in winter for the largest vertical scale motions at BIS (12<H_E<15 km) and at OHP (H_E≈30 km). During winter season, the potential energy density of the large-scale motions is found to be much larger at OHP than at BIS below 65-km altitude and nearly equal above. During equinoxes and summer, no significant difference appears between the energy levels of the large scale motions at both sites.

3.3. Power Spectral Density Versus Vertical Wave Number

The theoretical spectra versus vertical wave number, m, of a saturated gravity wave field is assumed to be proportional to m^{-t}, the spectral index t being, from dimensional arguments, equal to 3 [Dewan and Good, 1986]. The saturated spectral density is inferred by assuming that the amplitude of the waves is limited by the induced convective and/or dynamical instabilities [Dewan and Good, 1986; Smith et al., 1987; Sidi et al., 1988]. The normalized density fluctuations PSD versus vertical wave number, F(m), of a saturated wave field should thus be scaled as

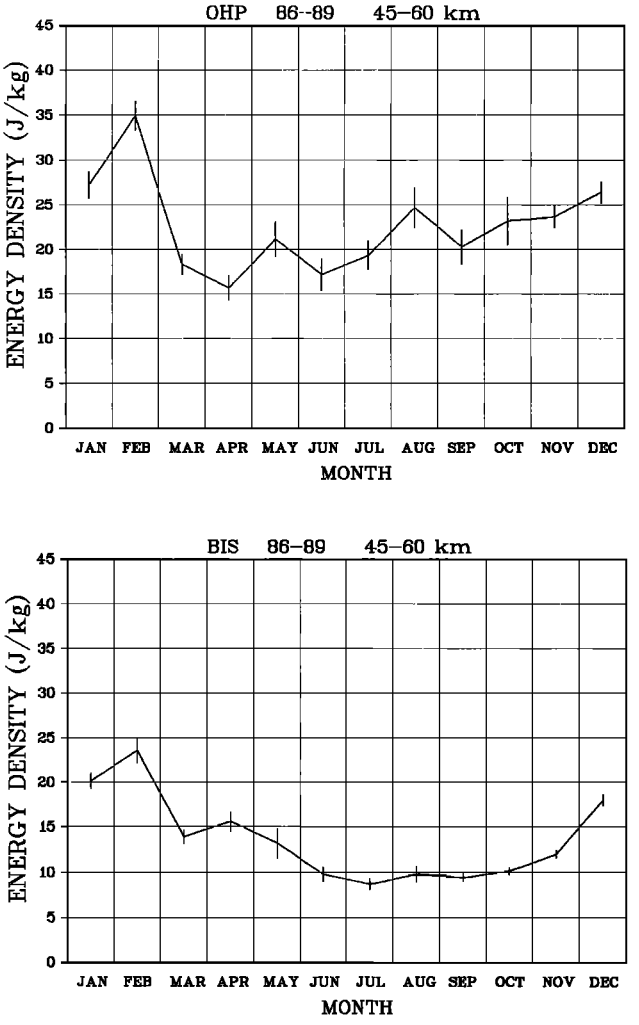

Fig. 6. The same as Figure 3 except in the lower mesosphere (45 to 60 km).

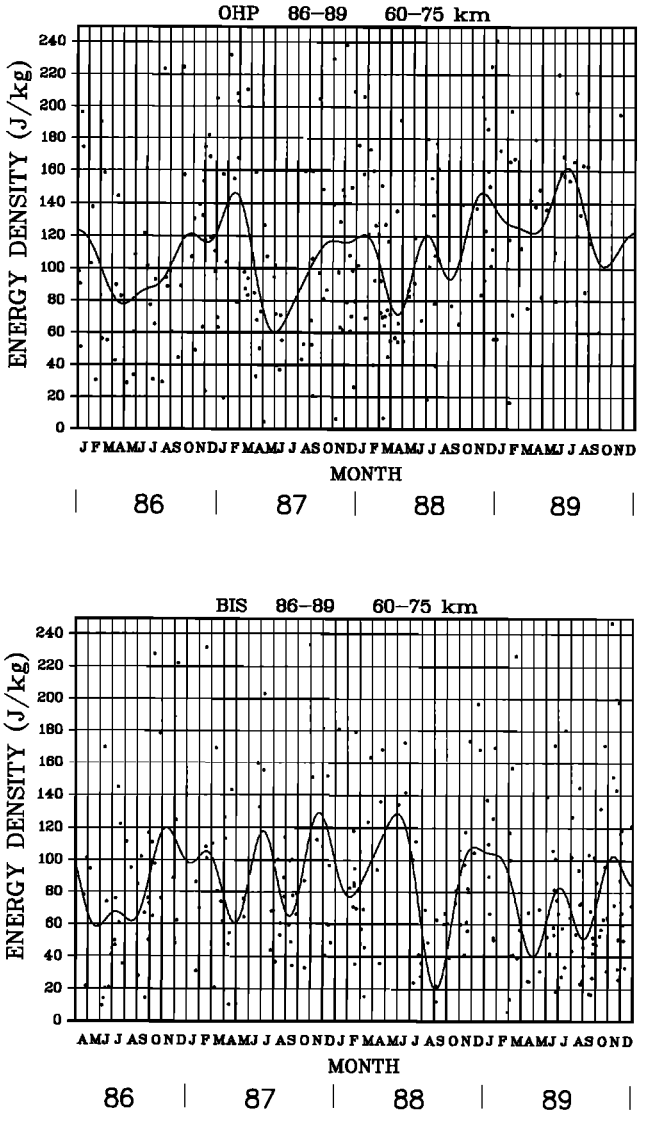

Fig. 7. The same as Figure 1 except in the middle mesosphere (60 to 75 km).

$$F^{s}_{(g/N^2)(\rho'/\rho_o)}(m) \approx \frac{\alpha}{m^3} \qquad (2)$$

where superscript s indicates saturation, α being a proportionality factor ranging from 1/2 [Dewan and Good, 1986] to 1/10 [Smith et al., 1987] depending upon the spectral width of the saturated range.

Figure 12 shows the monthly mean PSDs versus vertical wave number of the normalized density fluctuations $(g/N^2)\rho'/\rho_o$ in the upper stratosphere for 3 months at both sites. These PSDs are averaged over the spectra (deduced from 15-min integrated profiles) obtained during the months of January, July, and September from 1986 to 1989 (1987-1989 for January at BIS). The straight line proportional to m^{-3}, where m is the vertical wave number, indicates the convective saturation limit of equation (2) with α=1/2. The stratospheric PSDs are 1 or 2 orders of magnitude less than the convective limit (2) ($1/100<\alpha<1/10$) in the accessible spectral range (i.e., for vertical scales between 1 and 10 km). The spectral index, t, is generally larger than -3, ranging between -5/2 (in January) and -2 (in July and September). However, except during summer, the high wave number part of the spectra is, within the error bars, compatible with a -3 slope, α being then of the order of 1/20. Therefore the PSD of the short vertical scale fluctuations (less than 3 km) is consistent, within a factor of 2, with the saturation limit advanced by Smith et al. [1987]. Nevertheless, no definitive conclusion can be drawn from the density fluctuations measurements alone because saturation processes other than convective instabilities (dynamical instabilities or nonlinear interactions) could act to limit the waves' amplitude.

The normalized density fluctuation PSDs obtained in the lower mesosphere (45 to 60 km) for January, July and September are plotted in Figure 13. An increase by a factor of 3 to 10 of the PSD is observed from the upper stratosphere to the lower mesosphere in the entire accessible spectral range (1.5-2 to 10 km vertical scales), even though N^4 decreases by about a factor of 2 from the stratosphere to the mesosphere.

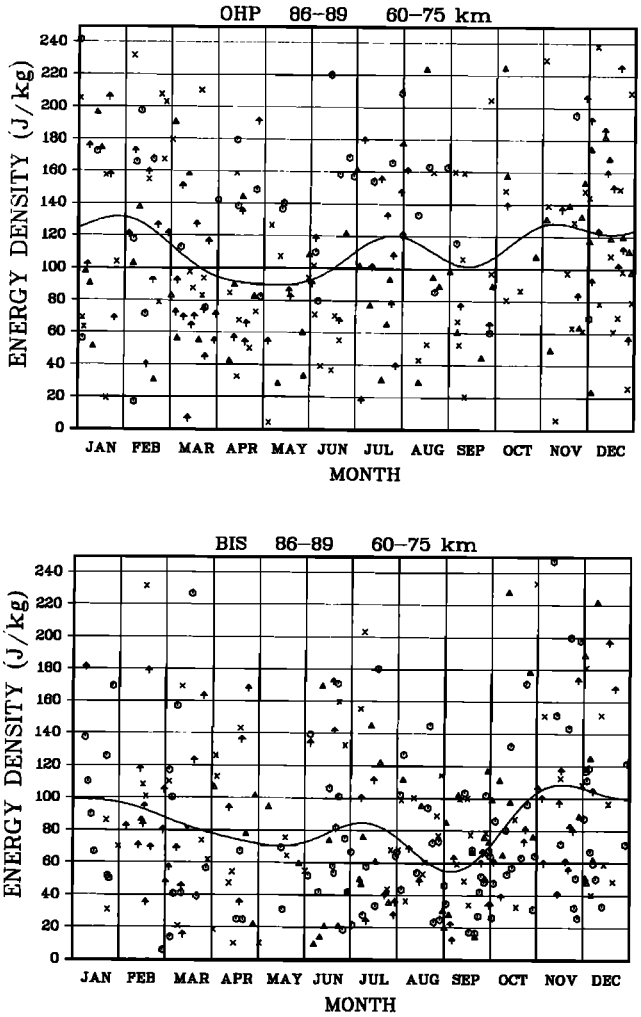

Fig. 8. The same as Figure 2 except in the middle mesosphere (60 to 75 km).

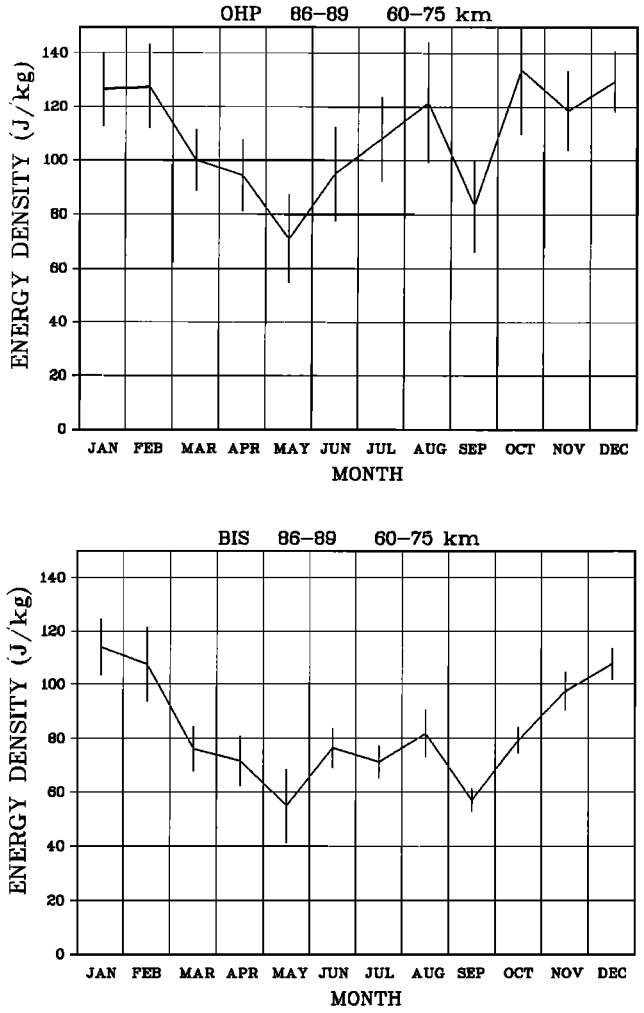

Fig. 9. The same as Figure 3 except in the middle mesosphere (60 to 75 km).

Such increasing PSD versus altitude suggests that the wave motions are not convectively saturated in the stratosphere (taking into account the chosen normalization of the density fluctuations a saturated PSD should stay constant). For large vertical scale motions (larger than 2 or 3 km), where the signal-to-noise ratio is relatively high, the spectral index is still larger than -3, ranging between -5/2 and -1. For the shortest vertical scale motions (less than 3 km) the PSD is close to the limit $1/2m^3$ ($1/4<\alpha<1/2$).

In the middle mesosphere (from 60 to 75 km altitude) the PSDs reach, or nearly reach, the convective limit $1/2m^3$ for vertical wavelengths up to 8 km in winter, and up to 4-5 km in summer and equinoxes (Figure 14). In the high wave number part of the spectra, a significant increase of the PSD is not observed as it was the case between the stratosphere and the lower mesosphere. This behavior for high wave numbers supports the hypothesis of a partially saturated wave field. The PSDs seem compatible with a -3 slope in the saturated range even though the errors bars may be too large to reach a definite conclusion. The gravity wave field appears convectively saturated above 60 km altitude, the upper vertical scales of the saturated range being larger during winter than during other seasons.

To summarize, the normalized density fluctuations PSDs obtained in the stratosphere and lower mesosphere indicate that the waves are not convectively saturated in the upper stratosphere (even though other saturation processes could limit the waves' amplitude). The standard deviation of the relative density fluctuations is less than 1% in the stratosphere. The PSD is close to $1/2m^3$ for wavelength up to

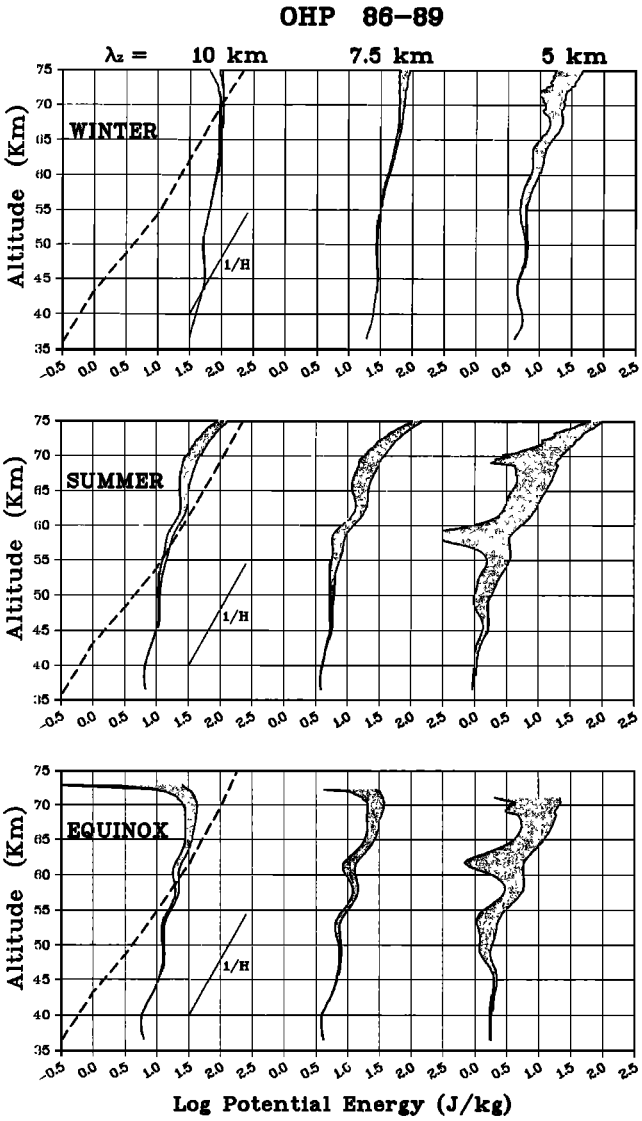

Fig. 10. The vertical growth of potential energy density per unit mass at OHP averaged over winter months (December, January, and February), summer months (June, July, and August), and "equinox" months (April, May, and September). The vertical growth of energy is deduced from a complex demodulation of the density fluctuations profiles in three wavelength bands centered at 10, 7.5, and 5 km. The noise variance, estimated by a demodulation of short vertical scales fluctuations (1 km and less), is plotted for comparison (dashed line).

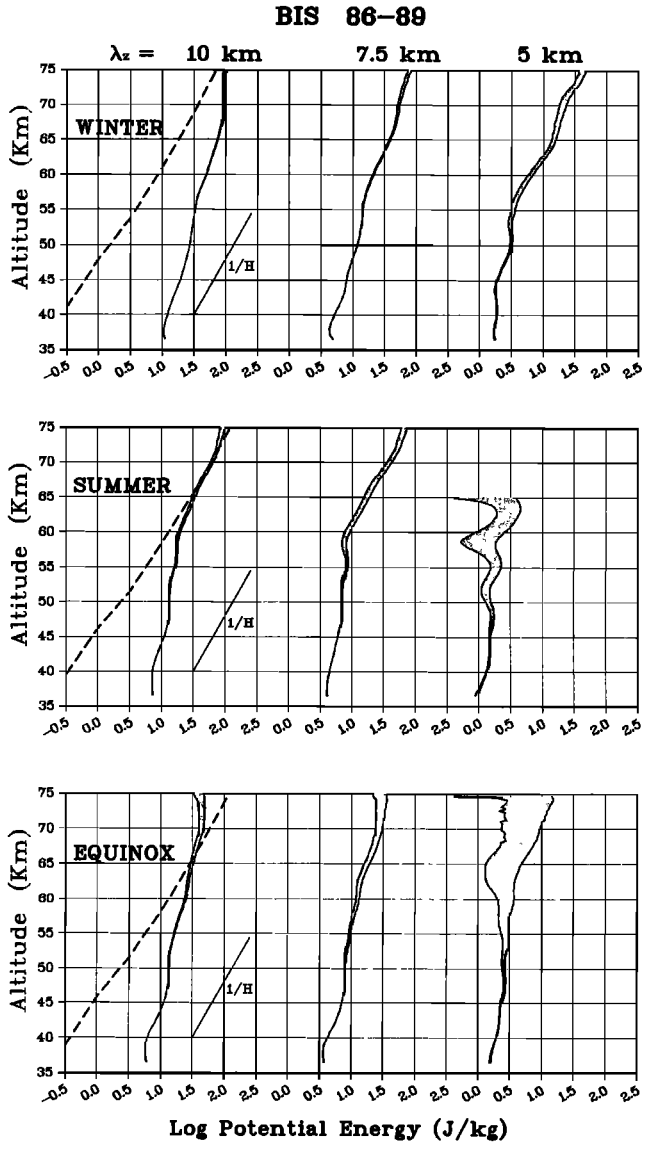

Fig. 11. The same as Figure 10 except at BIS.

3 km in the lower mesosphere, the standard deviation of the relative density fluctuations ranging between 1 and 2%. In the middle mesosphere, the wave field appears convectively saturated up to 6 to 8 km wavelength, the standard deviation of the relative fluctuations ranging between 2 and 3%. Therefore, assuming a partially saturated wave field, it appears that the larger vertical scale of the saturated range is, as suggested by Weinstock [1984] and Smith et al. [1987], an increasing function of altitude.

4. Discussion of Observations

4.1. Comparison With Other Climatological Studies

Up to present, the statistical studies of the gravity wave field characteristics and variability in the middle atmosphere result mainly from radar, rocket soundings and balloon borne instruments, and only a few from Rayleigh lidar. ST and MST radars have provided, up to now, the largest data base for gravity wave studies in the middle atmosphere, even though the altitude domain is limited to the lower stratosphere and upper mesosphere. Lidar and radar give access to different atmospheric parameters, respectively density (or temperature) and wind fluctuations, but with comparable space and time resolution (typically 5 to 20 min and 300 m in the mesosphere for MST radars). The wind and temperature fluctuations can be obtained simultaneously, but sporadically, by balloon-borne instruments (up to 25-km altitude) and rocket soundings (from 25- to 60-km altitude). Rayleigh lidar appears thus complementary with other sensing systems with regard to the accessible altitude range and to the atmospheric parameters they provide. Relevant results will be briefly recalled and compared with the ones presented here, even though they do not all concern the same height range and atmospheric parameters.

Statistical analyses of mesoscale wind and temperature fluctuations in the 30- to 60-km altitude range from rocket measurements have been performed by Hirota [1984], Hirota and Niki [1985] and Eckermann and Vincent [1989]. The first two of these studies lie on a data set obtained from 13 rocket stations, ranging in latitude from 8°S to 77°N during 6 years. The seasonal variability of the wave activity was found to be annual at high and middle latitude with winter maximum and summer minimum, grading to a semiannual variation at low latitude with equinoctial maxima [Hirota, 1984]. These findings are in general accord with those presented here, the annual cycle of the wave activity being clear below 60-km altitude. Furthermore, an energy scale height of 10 to 15 km was observed by Hirota and Niki [1985] and by Eckermann and Vincent [1989] as from lidar data (WCH and section 3.3 of this paper). A vertical anisotropy of the wave field was also found by these authors with predominantly upgoing wave energy. The lidar observations [WCH] show mostly downward vertical phase speeds (60 to 80% of the energy content) as expected for waves the energy of which propagates upward. It suggests that in most cases waves are generated below an altitude of 30 km.

Gardner and Voelz [1987], observing 171 monochromatic events, during 34 nights by mean of resonant lidar in the sodium layer (about 90-km altitude), do not find any significant seasonal variability of the gravity wave activity at mid-latitude.

Independently of the preliminary results obtained from the OHP data set [Chanin and Hauchecorne, 1981; Chanin et al., 1983], three studies of the gravity waves characteristics have been performed by Shibata et al. [1986, 1988] and Gardner et al. [1989] by using Rayleigh lidar. On the basis of 25 measurement nights, Shibata et al. [1986] have observed dominant low-frequency and large vertical wavelength modes in the 30- to 60-km altitude range at tropical latitude (33°N). A semiannual variability of the wave activity was also found, the maxima occurring during winter and summer. From case studies [WCH], the occurrence of low-frequency and large vertical wavelength modes was also observed quasi-systematically in the upper stratosphere and lower mesosphere

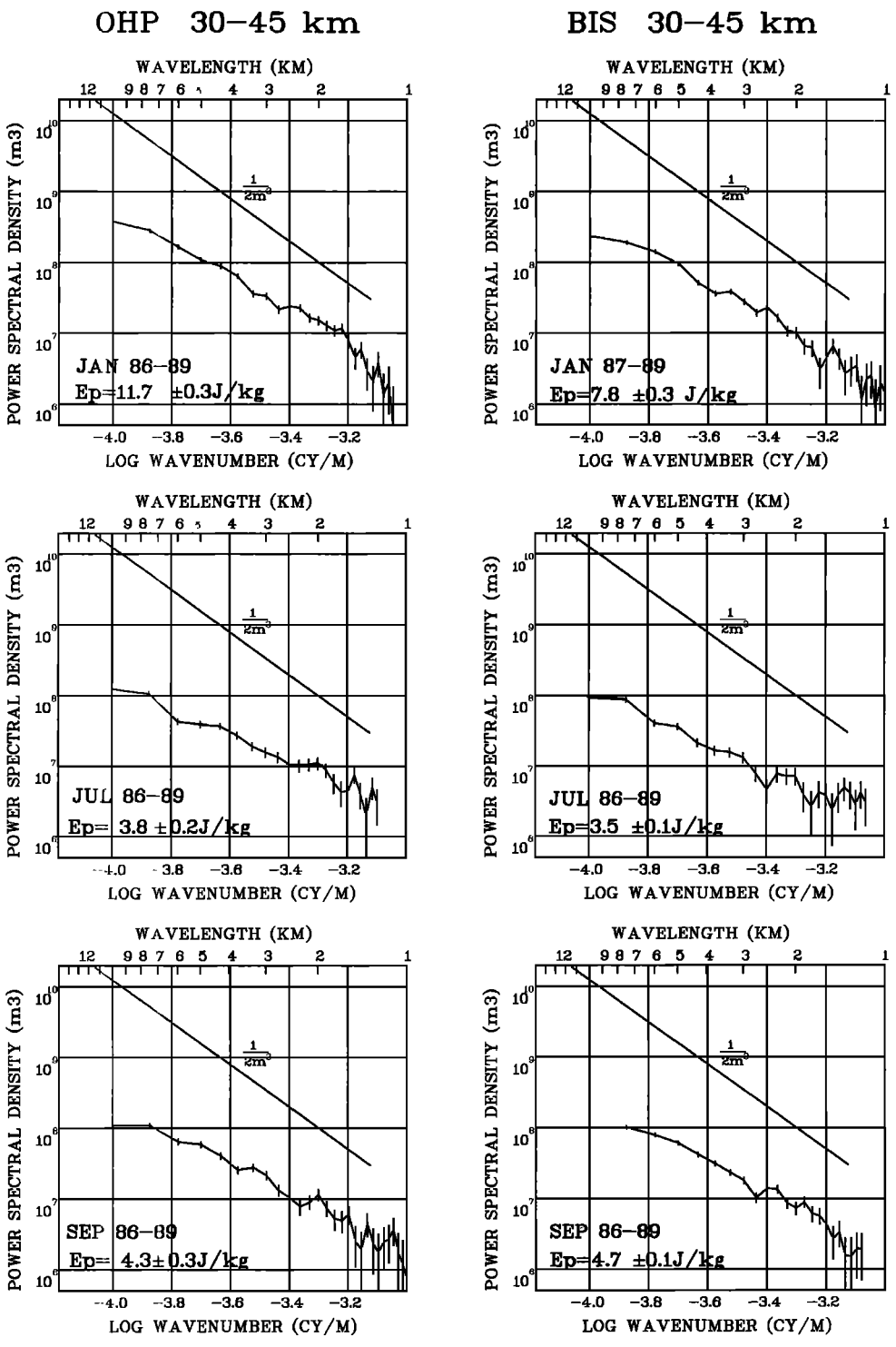

Fig. 12. The monthly means of the normalized density fluctuations PSD versus vertical wave number in the upper stratosphere (30 to 45 km) averaged over the spectra (resulting from 15 min integrated profiles) obtained during the January, July, and September months at OHP and BIS.

at OHP and BIS. These dominant inertia-gravity waves seem to be strongly damped in the mesosphere. On the other hand, we do not observe such a semiannual variation of the wave activity below 60 km. It indicates, as was suggested by Hirota [1984], that the seasonal variation of the wave activity varies with latitude. From the study of monochromatic wave events, observed during 13 measurement nights in the upper stratosphere, Gardner et al. [1989] found a clear increase of the vertical scales of the waves according to the observed period as well as an energy scale height of about 20 km,

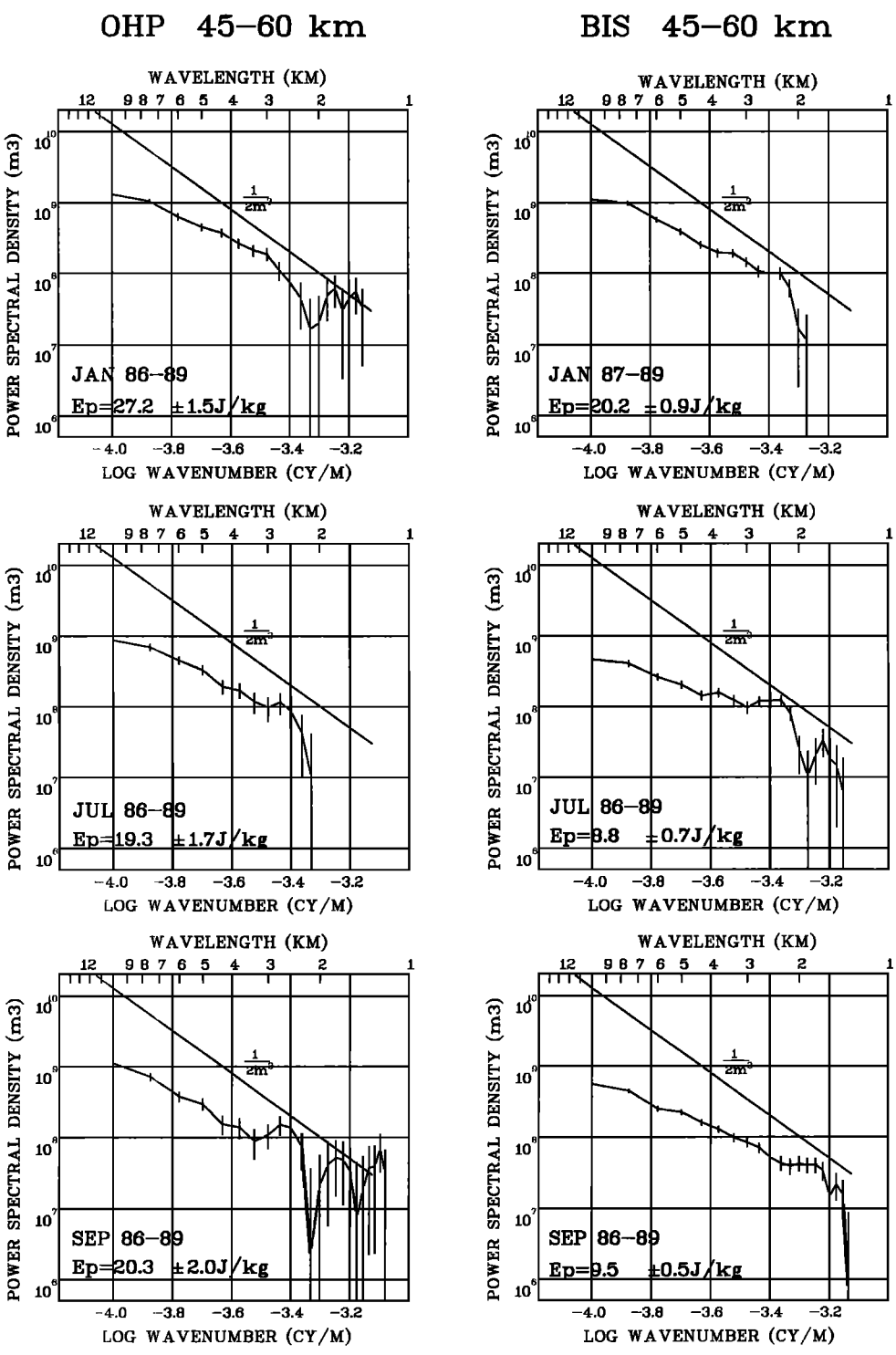

Fig. 13. The same as Figure 12 except for the lower mesosphere (45-60 km).

consistent with our findings. These authors do not observe any seasonal variation of the wave activity in the upper stratosphere.

The variance of the horizontal wind fluctuations in the high mesosphere, as observed by MST radars, shows a semiannual seasonal variation with equinoctial minima at Saskatoon (52°N) [Meek et al., 1985] and at Adelaide (35°S) [Vincent and Fritts, 1987]. An annual component of the wave activity is also observed from the MST radar data, the winter maximum of the wave activity being stronger than the summer one [Manson and Meek, 1986; Vincent and Fritts, 1987]. Manson and Meek [1986] have observed at Saskatoon a larger

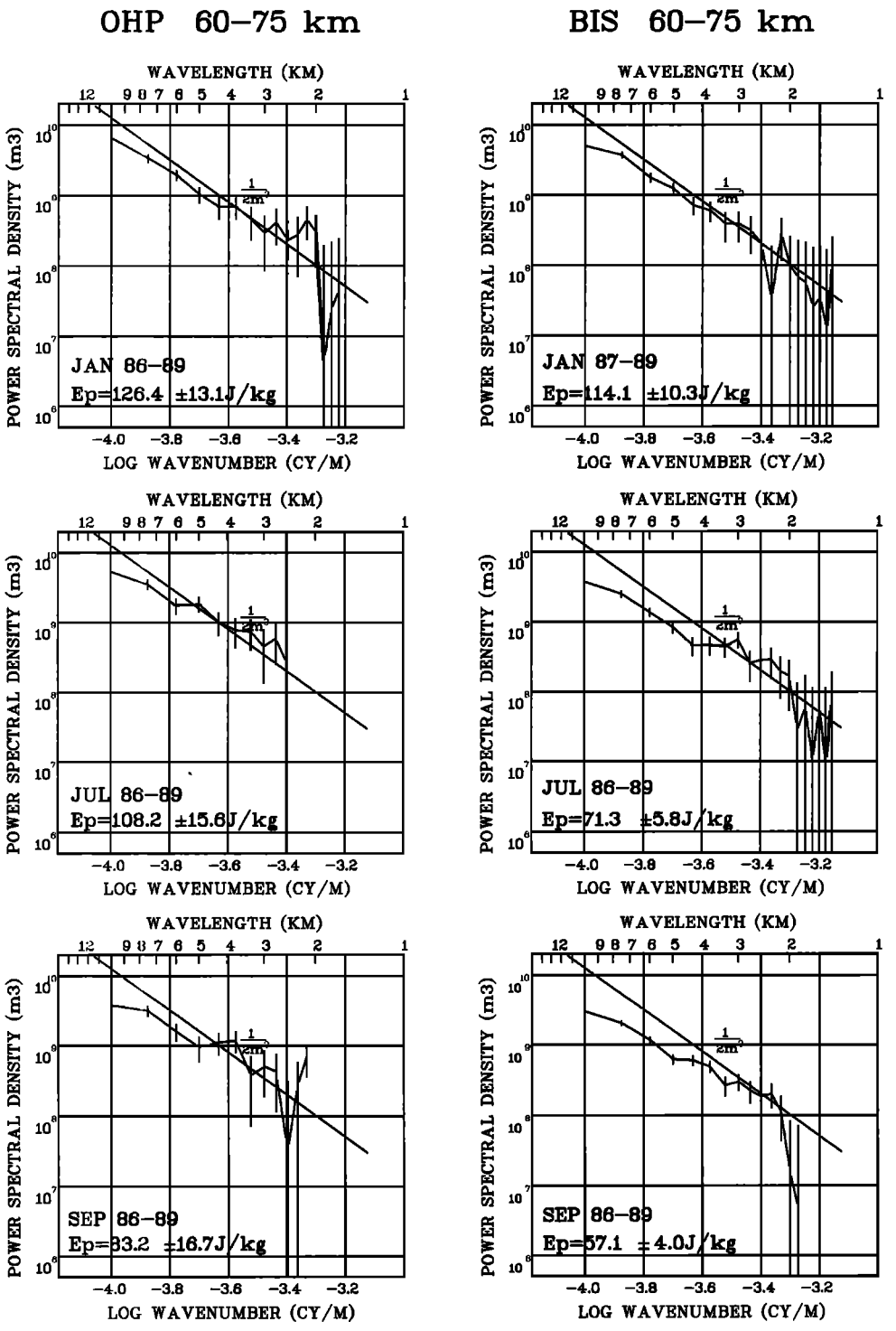

Fig. 14. The same as Figure 11 except for the middle mesosphere (60-75 km).

energy scale height during winter than during summer in the upper mesosphere. The results inferred from lidar data in the mesosphere, a semiannual variation as well as a larger energy scale height during winter (Figures 9, 10, and 11), are basically in agreement with these findings. Kinetic energy densities per unit mass at Saskatoon and Adelaide, ranging between 50 and 200 j/kg at 70-km altitude, are roughly of the same order of magnitude, even though slightly larger, than the potential energy density inferred from lidar data at mid-latitude in the 60- to 75-km height interval (from 60 to 130 j/kg).

As previously mentioned (WCH and section 3.3) we observe an increase of the density fluctuations PSDs versus

vertical wave number from the upper stratosphere to the lower mesosphere. A growth of a temperature PSD from the upper stratosphere to the lower mesosphere has also been observed by Shibata et al. [1988] (on the basis of 12 Rayleigh lidar profiles integrated from 2 to 5.5 hours). On the contrary, Smith et al [1987] and Tsuda et al. [1989] have shown, from in situ, ST and MST radar measurements, that horizontal wind PSDs are scaled with N^2 in the saturated range both in the stratosphere and mesosphere. Such an increase with altitude of the density (or temperature) PSDs is clearly in disagreement with the hypothesis of a saturated wave field because the power spectra are not scaled as N^4 from the stratosphere to the mesosphere. However, Fritts and Rastogi [1985] have advanced that low-frequency gravity waves should produce preferentially dynamical instabilities rather than convective instabilities, whereas higher-frequency modes should produce, nearly simultaneously, convective and dynamical instabilities. Now, the ratio of potential to kinetic energy depends upon the frequency distribution of the wave field. Using formula (1) and the polarization relationships

$$V' = -\,i\frac{f}{\omega}U' = \left(\frac{1-\omega^2/N^2}{\omega^2/f^2-1}\right)^{1/2}\frac{g}{N}\left(\frac{\rho'}{\rho_o}\right) \qquad (3)$$

the ratio of kinetic to potential energy, E_c/E_p, of a monochromatic wave can be written as

$$\frac{E_c}{E_p} = \frac{1+f^2/\omega^2}{1-f^2/\omega^2}\,(1-\omega^2/N^2) \qquad (4)$$

where U' and V' are the perturbation velocities in the direction of wave propagation and in the perpendicular direction respectively, $E_c=1/2(\langle U^2\rangle+\langle V^2\rangle)$. Therefore, gravity waves could be saturated producing dynamical instabilities (the horizontal wind PSD being then scaled as N^2/m^3) without producing convective instabilities, depending upon the frequency distribution of the wave field. The small PSD of the density perturbations in the stratosphere could be due to the relatively low frequency of the waves in this altitude domain [WCH]. Therefore the lidar and radar spectra may be compatible with regard to the saturation theory provided that the frequency distribution of the wave field is significantly different according to the altitude range. This point is discussed in more depth by Wilson et al. [1990].

4.2. Why is the wave activity variable?

Which processes could induce a seasonal variability of the wave activity having different characteristics following altitude range and location? The waves energy in the stratosphere is generally observed to propagate upward [Hirota and Niki, 1985; Eckermann and Vincent, 1989; WCH] suggesting that gravity waves are generated essentially in the troposphere and lower stratosphere. Therefore, assuming that wave sources are located essentially in the low atmosphere, the causes of such a variability could be, a priori, of three kinds. First, the intensity of the gravity wave sources (orography, ageostrophy, wind shears or convection) might greatly vary with time and location, depending on the topography, the planetary wave activity and/or other causes. The gravity wave generation processes are yet poorly known. Second, the intrinsic properties of the propagating waves (vertical and temporal scales), for a given set of initial characteristics (horizontal phase speed and direction of propagation), may vary according to the background flow. Third, the atmosphere could act as a selective filter, allowing or not the vertical propagation of the different wave modes.

The intrinsic characteristics of the waves (vertical wavelengths and frequency) are partly determined by the mean flow intensity and direction. Indeed, the intrinsic phase speed, c_i, can be written

$$c_i(z) = |\, c_h - \overline{u(z)}\cos\theta(z)\,| \qquad (5)$$

where $\overline{u(z)}$ is the mean horizontal wind intensity, c_h the horizontal phase speed of the wave and $\theta(z)$ the direction of the wave propagation with respect to the mean flow. The vertical wavelength, λ, and intrinsic frequency, ω, of a gravity wave are proportional to the intrinsic horizontal phase speed, c_i:

$$\lambda(z) = \frac{2\pi}{N(z)}\,c_i(z) = \frac{2\pi}{N(z)}\,|c_h - \overline{u(z)}\cos\theta(z)| \qquad (6)$$

$$\omega = k_h c_i(z) = k_h\,|c_h - \overline{u(z)}\cos\theta(z)| \qquad (7)$$

where k_h is the horizontal wave number.

The saturation amplitude of a single wave being proportional to its vertical wavelength, the altitude of saturation might be related to the vertical scale of the waves. Strong mean flow conditions are likely to favor the vertical propagation (without breaking) of the waves with relatively large intrinsic phase speed. Conversely, waves with low intrinsic phase speed are subject to a strong turbulent and/or radiative damping [Matsuno, 1982; Schoeberl and Strobel, 1984]. Moreover, according to the background wind profile and to the phase velocity of the waves, critical layers ($c_i=0$) induce a selective transmission of the vertically propagating waves [Lindzen, 1981]. The selective filtering may cause a prevailing direction of propagation of the waves against the mean flow. Such an horizontal anisotropy of the wave field in the middle atmosphere have been observed from MST radar observations [Vincent and Fritts, 1987] and rocket soundings [Eckermann and Vincent, 1989]. Therefore the mean atmospheric conditions largely induce the horizontal, vertical and temporal characteristics of the gravity wave field in the stratosphere and mesosphere. The temporal variability of the wave activity is now discussed having in mind these simple hypotheses.

Figure 15 shows the density fluctuations PSDs obtained at OHP and BIS in the upper stratosphere (30-45 km) and averaged over either winter months (January and February 1887-1989 and December 1986-1989), or summer months (June, July, and August 1986-1989). No significant

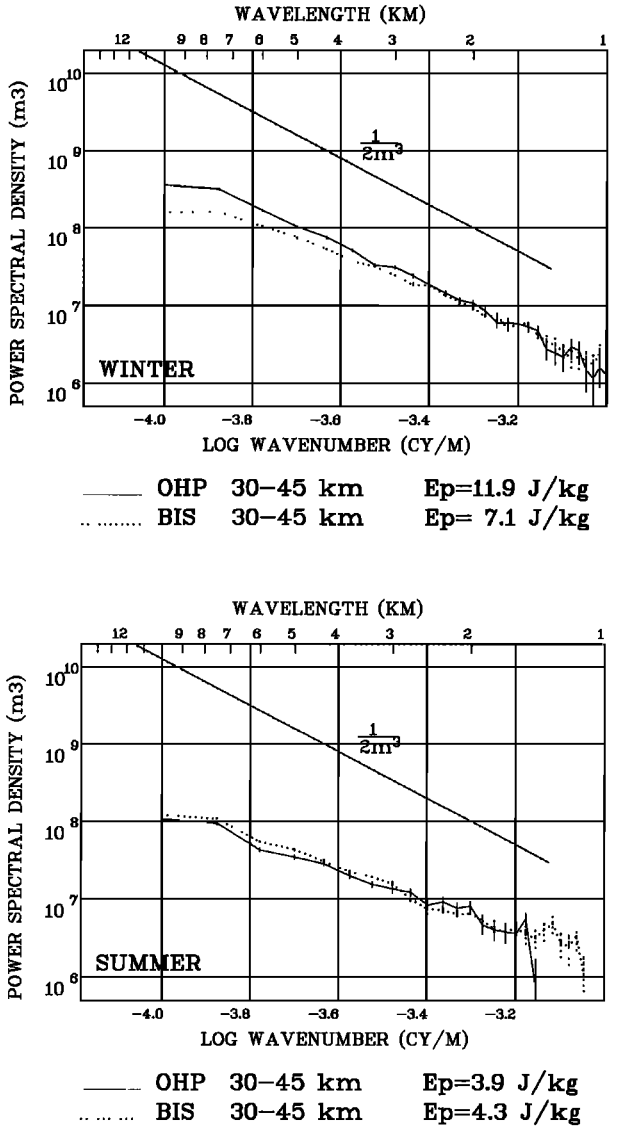

Fig. 15. The seasonal means of the normalized density PSDs at BIS and OHP are superimposed. The winter PSDs are averaged over the January, February (1987-1989) and December (1986-1989) spectra whereas the Summer PSDs are averaged over the June, July and August (1986-1989) spectra.

difference appears during summer, but the potential energy density is about 70% larger at OHP (11.9 j/kg) than at BIS (7.1 j/kg) during winter. More precisely, the winter PSD is found to be higher at OHP than at BIS for vertical scale motions larger than 3 km and nearly identical for smaller-scale motions. It has been also noticed, from demodulated profiles, that the variance of the large vertical scale fluctuations is much larger at OHP than at BIS during winter and almost the same during the other seasons (Figures 10 and 11). As was previously mentioned, it is likely that the orographic source is more intense at OHP, in the foothills of the Alps, than at BIS, on the Atlantic coast (where the dominant tropospheric flow is westerly). Now, orographic waves cannot propagate in summer owing to the wind reversal in the lower stratosphere. The energy density being quite similar at both sites during summer, the winter maximum of the wave activity, as well as as the difference of activity between the two sites observed during winter, are likely due to the vertical transmission of orographic waves. This clearly indicates that orography is a major gravity wave source.

It was noted in WCH that the dominant gravity wave modes have low apparent frequency, and thus relatively small horizontal phase speed (i.e., $c_h \sim 0$). Furthermore, it is reasonable to assume that the phase speeds of waves generated in the troposphere are of the same order of magnitude as the tropospheric flow. The vertical scale of the propagating waves is thus likely to be relatively large in case of strong wind intensity. On the other hand, the vertical wavelength of the waves reaching saturation is an increasing function of altitude (Figures 13 and 14). Therefore the equinoctial minima of the wave activity observed in the middle mesosphere could be a consequence of the relatively small vertical scales of the waves at time when the wind intensity is minimum, as such waves saturate at lower altitudes than waves of larger scale.

Assuming that the wave propagation is favoured by strong wind conditions, there should be a positive correlation between wind intensity and wave activity. The day-to-day correlation between the wind intensities at 50 and 2 mb and the energy densities per unit mass (Ep) in the 30- to 45-km and 60- to 75-km altitude range are shown in Figure 16. The wind intensities are obtained from the National Meteorological Center (NMC), interpolated above OHP, for the dates of lidar measurements during the year 1986. The 50- and 2-mbar levels have been chosen to represent the mean flow intensity below the two selected height ranges. The correlation coefficient, $\gamma = 0.73$, is significantly positive in the stratosphere. More than 50% ($\gamma^2 = 0.53$) of the day-to-day variability of the gravity wave activity in the stratosphere is simply related to the variation of the mean wind intensity. Above 60-km altitude the correlation is also positive ($\gamma = 0.42$) even though much less significant ($\gamma^2 = 0.18$).

Such simple hypotheses, as the selective transmission of the orographic waves and the dependency of the waves intrinsic characteristics upon the mean flow intensity, give an insight into the gross features of the wave activity variations. It is clear however that other processes such as the variability of the wave sources intensity in the low atmosphere, or the wave generation in the middle atmosphere itself (due to wind shears, instabilities or wave-wave interactions) are certainly not negligible. Nevertheless, the positive correlation between wave activity and wind intensity strongly supports the hypotheses that the waves characteristics, and thus the vertical propagation of the wave field, are largely induced by the background flow. The comparison of the energy densities observed at the two sites in the upper stratosphere during winter and summer clearly indicates that the annual variation of the wave activity is mainly due in this height range to the vertical transmission of orographic waves.

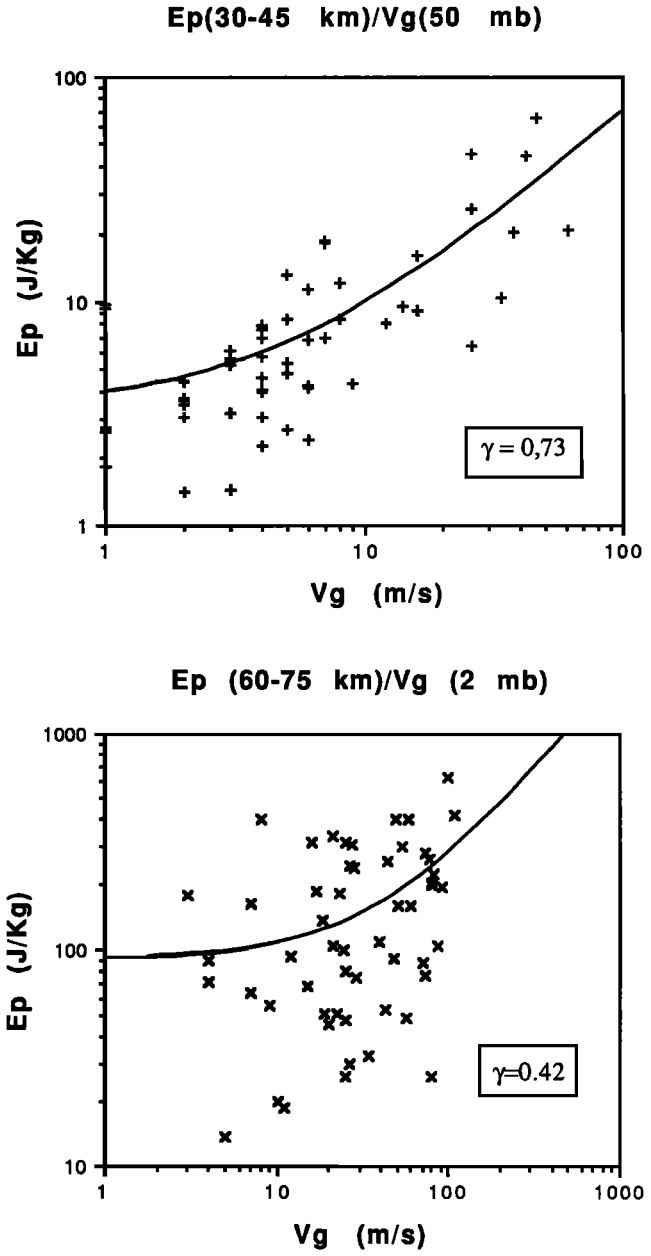

Fig. 16. Daily estimation of the potential energy density in the stratosphere (30 to 45 km) and mesosphere (60 to 75 km) versus mean wind intensity at 50 and 2 mb during year 1986. A positive correlation is observed in both cases.

5. Conclusions

The analysis of the mesoscale density fluctuations in the stratosphere and mesosphere from Rayleigh lidar data during 4 years (1986 to 1989) at OHP and BIS leads to the following conclusions:

1. The seasonal variability of the wave activity is essentially annual in the high stratosphere and low mesosphere, the maximum of activity occurring during winter, and the minimum during summer. A semiannual component is superimposed to the annual cycle above 60 km altitude, the two minima of activity occurring during the months of April-May and September, that is to say, when the mean wind intensity is weak. The amplitude of the seasonal variation, i.e., the difference between the energy density maximum and minimum, decreases with altitude (a factor of 2-3 in the upper stratosphere, and 1.5 to 2 in the middle mesosphere).

2. The energy density per unit mass is larger during winter at OHP than at BIS in the upper stratosphere, whereas no significant difference is observed during summer. As the orographic modes can not propagate during summer due to the stratospheric wind reversal and because the orographic source is likely to be more intense at OHP, the annual variation observed in the stratosphere may thus be due to the vertical transmission of orographic waves.

3. The potential energy density per unit mass is an increasing function of altitude. The energy scale height is generally larger than 10 km, suggesting an energy and momentum dissipation at all heights. The vertical growth of potential energy density varies with altitude range and season, smaller in the upper stratosphere than in the mesosphere, and larger in the mesosphere during summer than during other seasons.

4. The mean PSD versus vertical wave number of the density fluctuations is increasing from the stratosphere to the mesosphere. This fact strongly supports the hypothesis that the wave are not convectively saturated in the stratosphere in the accessible spectral domain (from 1 to 10 km wavelength).

5. The vertical scale of the waves reaching the convective saturation limit is a growing function of altitude in the mesosphere: the vertical scales of the waves reaching saturation ranges between 2 and 3 km in the lower mesosphere, between 5 and 8 km above 60-km altitude.

6. The wind intensity and the wave energy density are positively correlated in the stratosphere and mesosphere, indicating that the gravity wave activity is partially determined by the background flow.

The present findings are basically in agreement with the results obtained from other sources of data. Such a study of gravity waves in the middle atmosphere is the first extensive one using Rayleigh lidar data. By filling the gap between the low stratosphere and the high mesosphere (accessible to radars) it shows that the Rayleigh lidar is a powerful tool to monitor the gravity waves characteristics all along the path of their propagation into the middle atmosphere.

References

Chanin, M. L., and A. Hauchecorne, Lidar observation of gravity and tidal waves in the stratosphere and mesosphere, J. Geophys. Res., 86, 9715-9721, 1981.

Chanin, M. L., and A. Hauchecorne, Lidar studies of temperature and density using Rayleigh scattering, MAP Handbook, 13, edited by R. A. Vincent, pp. 87-99, SCOSTEP, Urbana, Illinois, 1984.

Chanin, M. L., A. Tarrago, and A. Hauchecorne, Planetary

and gravity waves as seen by lidar in the middle atmosphere, Proceeding VI ESA Symposium, Eur. Space Agency Spec. Publ., ESA SP 183, 175-179, 1983.

Dewan, E. M., and R. E. Good, Saturation and the "universal" spectrum for vertical profile of horizontal scalar winds in the stratosphere, J. Geophys. Res., 91, 2742-2748, 1986.

Eckermann, S. D., and R. A. Vincent, Falling sphere observations of anisotropic wave motions in the upper stratosphere over Australia, Pure Appl. Geophys., 130, 509-532, 1989.

Fritts, D. C., and P. K. Rastogi, Convective and dynamical instabilities due to gravity wave motions in the lower and middle atmosphere: Theory and observation, Radio Sci., 20, 1247-1278, 1985.

Garcia, R. R., and S. Solomon, The effects of breaking gravity waves on the dynamical and chemical composition of the mesosphere and lower thermosphere, J. Geophys. Res., 90, 3850-3858, 1985.

Gardner, C. S., and D. G. Voelz, Lidar studies of the nighttime sodium layer over Urbana, Illinois, 2,. Gravity waves, J. Geophys. Res., 92, 4673-4694, 1987.

Gardner, C. S., M. S. Miller, and C. H. Liu, Rayleigh lidar observations of gravity wave activity in the upper stratosphere at Urbana, Illinois, J. Atmos. Sci., 46, 1838-1854, 1989.

Hauchecorne, A., and A. Maillard, A 2D dynamical model of mesospheric temperature inversions in winter, Geophys. Res. Lett., 17, 2197-2200, 1990.

Hauchecorne, A., M. L. Chanin, and R. Wilson, Mesospheric temperature inversion and gravity wave breaking, Geophys. Res. Lett., 14, 933-936, 1987.

Hirota, I., Climatology of gravity waves in the middle atmosphere, J. Atmos. Terr. Phys., 46, 767-773, 1984.

Hirota, I., and T. Niki, A statistical study of inertia gravity waves in the middle atmosphere, J. Meteorol. Soc. Jpn., 63, 1055-1066, 1985.

Holton, J. R., The role of gravity wave-induced drag and diffusion in the momentum budget of the mesosphere, J. Atmos. Sci., 39, 791-799, 1982.

Lindzen, R. S., Turbulence and stress due to gravity wave and tidal breakdown, J. Geophys. Res., 86, 9707-9714, 1981.

Manson, A. H., and C. E. Meek, The dynamics of the mesosphere and lower thermosphere at Saskatoon (52°N), J. Atmos. Sci., 43, 276-284, 1986.

Matsuno, T., A quasi-one-dimensional model of the middle atmosphere circulation interacting with gravity waves, J. Meteorol. Soc. Jpn., 60, 215-226, 1982.

Meek, C. E., I. M. Reid, and A. H. Manson, Observation of mesospheric wind velocities, 2, Cross sections of power spectral density for 48-8 h, 8-1 h, 1 h-1 min over 60-110 km for 1981, Radio Sci., 20, 1383-1402, 1985.

Miyahara, S., Y. Hayashi and J. D. Mahlman, Interactions between gravity waves and the planetary scale flow simulated by the GFDL "SKYHI" general circulation model, J. Atmos. Sci., 43, 1844-1861, 1986.

Palmer, T. N., G. J. Shutts, and R. Swinbanck, Alleviation of a systematic westerly bias in general circulation and numerical weather prediction through an orographic gravity wave drag parameterization, Q. J. R. Meteorol. Soc., 112, 1001-1040, 1986.

Schoeberl, M. R., and D. F. Strobel, Nonzonal gravity wave breaking in the winter mesosphere, in Dynamics of the Middle Atmosphere, edited by J.R. Holton and T. Matsuno, pp. 45-64, Terra, Tokyo, 1984.

Shibata, T., T. Fukuda, and M. Maeda, Density fluctuations in the middle atmosphere over Fukuoka observed by an XeF Rayleigh lidar, Geophys. Res. Lett., 13, 1121-1124, 1986.

Shibata, T., S. Ichimori, T. Narikiyo, and M. Maeda, Spectral analysis of vertical temperature profiles observed by a lidar in the upper stratosphere and the lower mesosphere, J. Meteorol. Soc. Jpn., 66, 1001-1005, 1988.

Sidi, C., J. Lefrère, F. Dalaudier, and J. Barat, An improved atmospheric buoyancy wave spectrum model, J. Geophys. Res., 93, 774-790, 1988.

Smith, S.A., D. C Fritts, and T. E. Van Zandt, Evidence of a saturated spectrum of atmospheric gravity waves, J. Atmos. Sci., 44, 1404-1010, 1987.

Strobel, D. F., J. P. Apruzese, and M. R. Schoberl, Energy balance constraints on gravity wave induced eddy diffusion in the mesosphere and lower thermosphere, J. Geophys. Res., 90, 13067-13072, 1985.

Tanaka, H., A slowly varying model of the lower stratospheric zonal wind minimum induced by mesoscale mountain wave breakdown, J. Atmos. Sci., 43, 1881-1892, 1986.

Tsuda, T., T. Inoue, D. C. Fritts, T. E. Van Zandt, S. Kato, T. Sato, and S. Fukao, MST radar observation of a saturated gravity wave spectrum, J. Atmos. Sci., 46, 2440-2447, 1989.

Vincent, R. A., and D. C. Fritts, A climatology of gravity wave motion in the mesopause region at Adelaide, Australia, J. Atmos. Sci., 44, 748-760, 1987.

Weinstock, J., Gravity wave saturation and eddy diffusion in the middle atmosphere, J. Atmos. Terres. Phys., 46, 1069-1082, 1984.

Wilson, R., A. Hauchecorne, and M. L. Chanin, Gravity wave spectra in the middle atmosphere as observed by Rayleigh lidar, Geophys. Res. Lett., 17, 1585-1588, 1990.

Wilson, R., M. L. Chanin, and A. Hauchecorne, Gravity waves in the middle atmosphere observed by Rayleigh lidar, 1, Case studies, J. Geophys. Res., this issue.

M. L. Chanin, A. Hauchecorne and R. Wilson, Service d'Aéronomie du CNRS, 91373 Verrières le Buisson Cedex, France.

(Received December 19, 1989;
revised November 26, 1990;
accepted November 26, 1990.)